CHAPTER 42
FLIXBOROUGH: THE DISASTER AND ITS AFTERMATH

J. E. S. Venart
Department of Mechanical Engineering,
University of New Brunswick, Fredericton,
New Brunswick, Canada

If we do not understand the past we cannot make proper sense of the present or the future.

42.1 BACKGROUND

On June 1, 1974, a fire and massive explosion occurred at the Nypro (UK) Ltd. works near Flixborough, North Lincolnshire (Fig. 42.1). An accidental release of cyclohexane at 0.96 MPa and between 150 to 155°C resulted in an unconfined vapor cloud explosion (UVCE) that caused 28 fatalities, the destruction of the plant, severe injury to inhabitants, and sig-

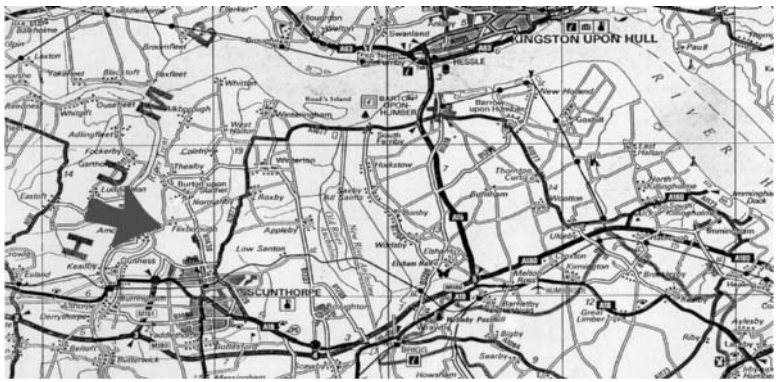

FIGURE 42.1 Map of the Humber River and surroundings. The plant location is indicated by the arrow.

nificant damage to many buildings in the surrounding countryside (Secretary of State for Employment, 1975).

The plant was located on the east bank of the River Trent, a tributary of the Humber, about 50 km west of the fishing port of Grimsby. On the west bank of the river, opposite the NYPRO site, was the village of Amcotts; the village of Flixborough was on a small rise to the East; the town of Scunthorpe was southeast of the location. All suffered major distress though no loss of life.

The catastrophe was initiated in section 25A of the process stream (Fig. 42.2) during start-up while the cyclohexane feedstock, inerted with nitrogen, was under hot recycle through the reactor train, R1 to R6. Only about one-third of the 70 kg/s full production flow was recirculating at the time.

A portion of the plant is shown in Fig. 42.2. Section 25A was south and midway between the laboratory and the works and main office buildings. Adjacent was section 7 (the caprolactam plant) and section 27. The reactor train (R1 to R6), which was considered the source of the release, was aligned primarily north-south. A temporary 20-in. (0.5-m) pipe assembly bridged reactors R4 and R6, and the removed reactor, R5, had been placed in waste ground in front of the works office and alongside of the section. At the time the wind was blowing to the northeast at about 4 to 6 m/s. Shown also is an estimated outline of the flammable cloud. The perceived center of the explosion, as determined by several investigators, was identified as being at the roadway just in front of the main office.

In the oxidation sequence there had been six reactors (Fig. 42.3). However, the fifth reactor, R5, had been removed because of damage and a temporary 304L stainless steel (SS) 0.5-m diameter pipe bridge, which used the two original 0.71-m diameter bellows (B) and 316L SS stub pipe (P) assemblies, had been installed between R4 and R6.

The reactors were made of 13-mm steel with a 3-mm thick SS steel liner. Each was about 5 m high by 3.5 m in diameter and was fitted with an interior overflow weir and baffle plate to ensure level control and bottom feed, proper oxidation, and mixing. All but one, R4, had an agitator (Artingstall, 1974).

The original 0.71-m interconnecting pipes and their bellows had permitted the hot pressurized feedstock to communicate by open channel flow over the outlet weir in the upstream reactors, through the bellows connection into the downstream reactors with a fixed difference in elevation of 0.178 m and at a velocity of less than 0.3 m/s through the nearly full pipes under full production flow. The adaptation (Fig. 42.4), however, doubled the head between R4 and R6 to 0.356 m. There was also a significant weir ''waterfall'' (velocities from 1.8 to

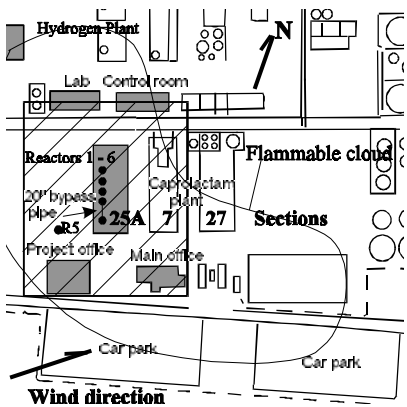

FIGURE 42.2 Portion of the Nypro site plan showing section 25A and the reactor train.

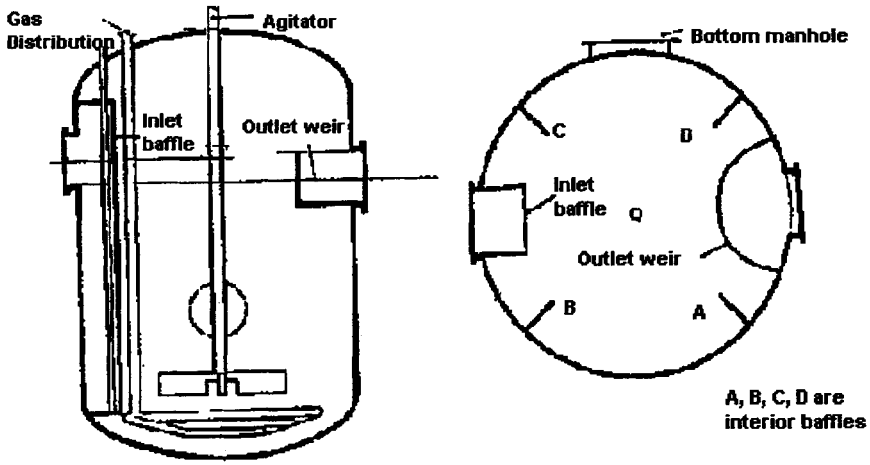

FIGURE 42.3 Reactor vessel details; elevation and plan views. (*Source: Artingstall, 1974.*)

2.6 m/s) in addition to two hydraulic jumps in the very complex flow structure (Fig. 42.5). In the R4 to B4 section, the 0.71-m pipe was now nearly half full and under full production the velocity would have been about 0.5 m/s. Immediately after the transition into the 0.5-m section, the flow accelerated and became supercritical, ending in a significant hydraulic jump near the lower miter bend, with flow slugging into the lower B6 bellows and thence into R6. Here the flow was quiescent and filled the rest of the 0.5-m pipe (velocity at full production about 0.3 m/s) (Teng-yang et al., 2000).

The modification made was thus more than just a geometric alteration. Significant changes were made to the statics, the dynamics, and the flow in the assembly. First, due to the differences in diameter and the dogleg shape, we have a couple which loads the pipe latterly in the vertical direction. Second, we have a mass spring system with very little support

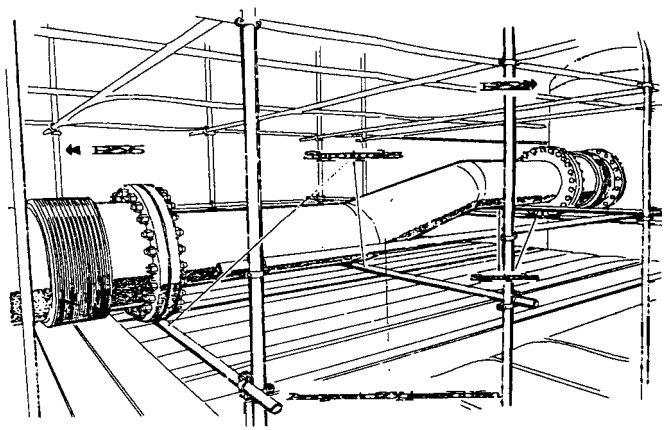

FIGURE 42.4 Reconstruction of the R5 bypass assembly showing the two 0.71-m diameter bellows and stub pipes, the 0.5-m dogleg pipe, and the support scaffolding used. (*Source: Secretary of State for Employment, 1975.*)

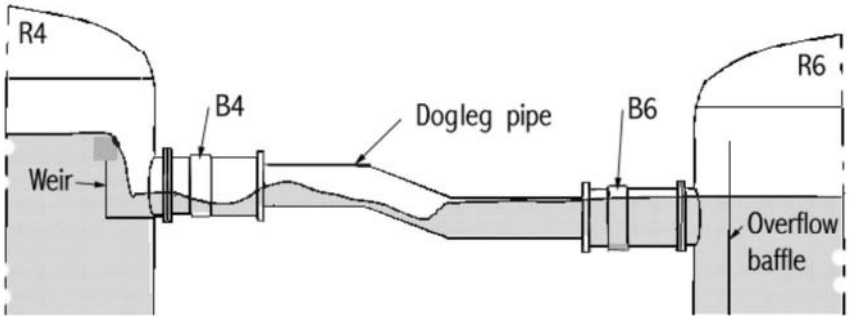

FIGURE 42.5 Reactor train vessels R4 to R6 with the temporary bypass pipe with the liquid levels as for full flow. (*Source: Teng-yang et al., 2000.*)

provided by the scaffolding, especially upon vertical thermal expansion of the reactors. And finally, there are the significant discharge and flow alterations noted earlier.

Each bellows had a first natural frequency of about 65 to 71 Hz axially and between 325 to 416 Hz in the transverse direction; the system frequency, as determined for a straight pipe, was 3.9 Hz axial, 15.7 Hz lateral (ends of the spool pipe in phase), and 27.2 Hz for the rocking mode.

The excitation of this very complex spring-mass system was now such that resonances with the flow were possible (Teng-yang et al., 2000). Most of the lower frequencies could have been excitable by the very broad range of flow velocities present, particularly near the two hydraulic jumps (EJMA, 1993). Additionally, the jetting at the base of the weir outfall could possibly result in axial resonance of the bellows. Coherent turbulence may also have been able to excite the higher modes.

With flow-induced vibration, no significant response is observed up to some critical velocity, and then, as the velocity is increased further, the bellows can become unstable. For uniform mean flows the critical Strouhal number[1] is St = 0.45 (Weaver and Ainsworth, 1989); for nonuniform flows, as at the exits of elbows leading to bellows and perhaps the weir outfall region, St = 0.57 (Jakubauskas and Weaver, 1998a, b).

The flexibility of expansion joints makes them susceptible to self-excited vibration, resulting in bending stresses that may produce fatigue failure (Weaver and Ainsworth, 1989). Gigacycle[2] fatigue damage to the thin wall (~1-mm thick: Foley, 1974a) 12-convolution bellows could well have occurred since between 64 to over 300 million cycles could have been possible within the range of potential excitations present during the two-month operating period. Indeed, it had already been noted that the assembly was unstable as it lifted off its supports during operation (Secretary of State for Employment, 1975).

The process fluid, Cyclohexane (C_6H_{12}, MW 84) is a colorless liquid similar in some of its properties to gasoline (flash point 20°C, auto-ignition temperature (AIT) 245°C). The fluid has a normal boiling point of 80°C and a saturation pressure, p_{sat}, at 150°C of 0.55 MPa. When the liquid was saturated with nitrogen, or air as when oxidation was occurring in the reactor stream, the pressure was 0.96 MPa. Under these conditions the liquid was 99.8% C_6H_{12} and 0.2% N_2 or air; the vapor would have consisted of 82.6% C_6H_{12} and 17.4% N_2

[1] St $(fp)/V$, where f is the bellows natural frequency in Hz, p is the bellows pitch (m), and V is the mean flow velocity (m/s).

[2] The fatigue testing of steels usually stops before 100 million cycles since a fatigue limit is registered between 1 and 10 million cycles. However, tests conducted with high-frequency random vibration (similar to those associated with the natural resonance of a structure) show that the fatigue limit of steels disappears and that fatigue failures occur (Miller, 1999; Au-Yang, 1999).

FIGURE 42.6 Looking north over the rubble of the main office building into section 27. (*Photograph courtesy the Scunthorpe Evening Telegraph.*)

or air. The bubble point pressure of this mixture, p_{sat}(150°C), was 0.956 MPa. The lower flammable (LFL) and upper flammable limits (UFL) of a vapor–air mixture by weight under atmospheric conditions are 3.46 and 19.8 wt % (1.3 vol. %; 7.8 vol. %), respectively.

The scale of the disaster and damage can be appreciated from photographs taken soon after the explosion and shown in Figs. 42.6 and 42.7.

In Fig. 42.6 we are looking north over the rubble of the main office building at section 27. Notice the crushed columns to the right of the section and the (amazingly) still near-vertical lamppost, all indicators that this location was near the center of the explosion. Note also that the columns and vessels on the west (left) side of the section and to the north are uncrushed.

In Fig. 42.7 the parking lot to the southeast of the main office building is shown. This spot is near where the main entrance and gate house would earlier have been. In the background, notice the overturned tanker truck (estimates of the pressures necessary to crush its tank range up to 1 MPa: Gugan, 1978). Note that the vehicles in the parking lot have been shredded, also indicative of extremely large overpressures.

42.2 THE COURT OF INQUIRY

An Official Court of Inquiry was immediately appointed by the Secretary of State for Employment, Michael Foot, ''to establish the causes and circumstances of the disaster and to point out any lessons . . . to be learned therefrom.'' The essential problem faced by the Court was ''to determine what had caused the rupture of the by-pass.'' The possibilities investigated were: ''i) rupture of the by-pass assembly through internal pressure; ii) rupture of the assembly in two stages; a *small tear in the bellows* (bellows B4) leading to an escape and a minor explosion causing final rupture; and iii) rupture of the '8 inch' line at the 50-inch split leading also to a minor explosion causing rupture of the by-pass assembly.''

FIGURE 42.7 The Nypro parking lot to the southeast of the main office building. (*Photograph courtesy of the Scunthorpe Evening Telegraph.*)

Processes ii) and iii) were interpreted to require *external* minor explosions to trigger events; no physical evidence for these could be determined. Despite the physical evidence of the internal tear in bellows B4 (Foley, 1974a) and compelling eyewitness evidence, only three paragraphs in the final report and a few pages in the Court's record and *no* definitive studies were devoted to the consideration of the two-stage rupture possibility that would have included the likelihood of a fatigue-induced initiation to the sequence of events. Only processes i) and iii) were examined in depth, with nearly 50% of the Report of the Inquiry, the Record of the Court, and the supporting studies being devoted to the consideration of one or the other of these cases. Other possibilities considered for an *internal* initiating event (e.g., peroxide decomposition and the operation of a nitrogen purge) were excluded. The likelihood of a water/cyclohexane superheated explosive boiling interaction (King, 1975, 1977) was also not considered, and recent experiments undertaken by the U.K. Health and Safety Executive (HSE) on behalf of the Minister of the Environment (King, 1999), could suggest what role, if any, water trapped in the bottom of one of the reactors may have played in the event.

On the basis of expert evidence by Professor D. E. Newland (1976) based on a dynamic analysis and assessment of energy requirements for both bellows to squirm and the bypass pipe to buckle as one event, the Court concluded, albeit with *low probability*, ''that the disaster resulted from a one stage failure of the 20-inch assembly'' as a result ''of conditions of pressure and temperature more severe than any which had previously prevailed but no higher than careful and conscientious plant operators could be expected to permit.'' The Court did, however, state that this conclusion ''would be readily displaced if some [other event of] greater probability to account for the rupture could be found'' (Secretary of State for Employment, 1975).

Extensive full-scale experiments were undertaken in attempts to reproduce the failure (Games and Waterhouse, 1974; Batstone, 1975). These employed a similar pipe assembly (as shown in Fig. 42.4) as well as other experiments and bellows tests evaluated at the same and more severe operating conditions. All these experiments were unable to reproduce the failure process accepted.

In view of the Court of Inquiry's qualified conclusion, the cause of the accident has been the subject of considerable controversy, especially as to the actual failure process (e.g., Ball, 1975, 1976; Butler, 1975; Cox, 1976; Gugan, 1976; King, 1977; Warner, 1975; Warner and Newland, 1975); the amount of cyclohexane released, and whether the unconfined vapor cloud formed in the release detonated (e.g., Gugan, 1978, 1980; Ale and Bruning, 1980a, b; Fu and Eyre, 1980; Phillips, 1981). The debate and argument continue to this day (e.g., Gugan, 2000; Hoiset et al., 2000; King, 2000; Kletz, 2000; Swan, 2000).

In the present reanalysis, the bellows, the bridging pipe, and its assembly into the bypass are modeled and a release scenario that considers the likely sequence of events initiated by the crack noted by the Court in possibility ii) above is advanced. These considerations utilize finite-element analyses (FEA) of the bellows and pipe assembly as well as computational fluid mechanics (CFD) models of the two potential release secenarios: that accepted by the Court and the one considered here. The results of both examinations demonstrate that the proposed two-step failure of the pipe bridge is more probable based on the physical and eyewitness evidence available. The localized explosion damage additionally supports the conclusion that the cloud was detonated.

42.3 INTRODUCTION

The initiating mechanism proposed first requires an initiating tear near the top of the upstream, B4, bellows. This bellows was the only one that was found with an internal tear (Secretary of State for Employment, 1975; Foley, 1974a) in the areas of the bellows most highly stressed; i.e., near the topmost convolutions of the bellows closest to R4 (Venart and Tan, 2000).

The various steps in the failure process are detailed in Fig. 42.8 with a tabulation of the sights and sounds that would have been experienced in Table 42.1. The very complex process can be summarized as follows:

- The instability of the assembly and the near resonance of the upstream, B4, bellows with the forcing fluid flow initiates fatigue damage, which accumulates in the most highly stressed, and least damped, regions of the unit.
- Sufficient damage accumulates to cause a tear, which further opens, due to pressure, and local vapor-gas depressurization occurs (Fig. 42.8*a*). There is a bang and a sound like a pressure relief valve going off (Table 42.1).
- B6 next rapidly expands and B4 compresses due to this unequal pressure distribution (Fig. 42.8*b*), and the now superheated and supersaturated cyclohexane rapidly (~50 ms) boils up. The impact of this two-phase swell results in a head-space impact and dynamic re/overpressurization (Gromles, 1984; Venart and Ramier, 2000). This immediately causes both the compression of the downstream, B6, bellows *and* the initiation of upwards 'squirm' of the B4 bellows (Fig. 42.8*c–e*). First there is a thud as B4 is compressed, and then a minor rumbling of the boiling process in the B4 region of the pipe bridge, and then a further thud as B6 is compressed by the repressurization occurring near B4 (Table 42.1).
- The compression of B6 by this local overpressure constrains the dogleg pipe at its R6 connection (Snedden, 1985) and causes the process of B4 squirm to act over the full 356-mm eccentricity (Fig. 42.8*d*) with much less force than that required for the 178-mm offset required in Newland's single-stage analysis (Newland, 1976).
- This process results in the commencement of collapse by buckling of the 0.5-m pipe as the B4 bellows continues to squirm, then balloon, burst and rip off *at its normal operating pressure* due to the p-V work of the expanding two-phase fluid (Fig. 42.8*f*).
- The ripped off topmost section of the bellows by this process is projected upwards and sails into the air and appears to some (Harry, 1974), as a blown-off ''tank top''; it is found

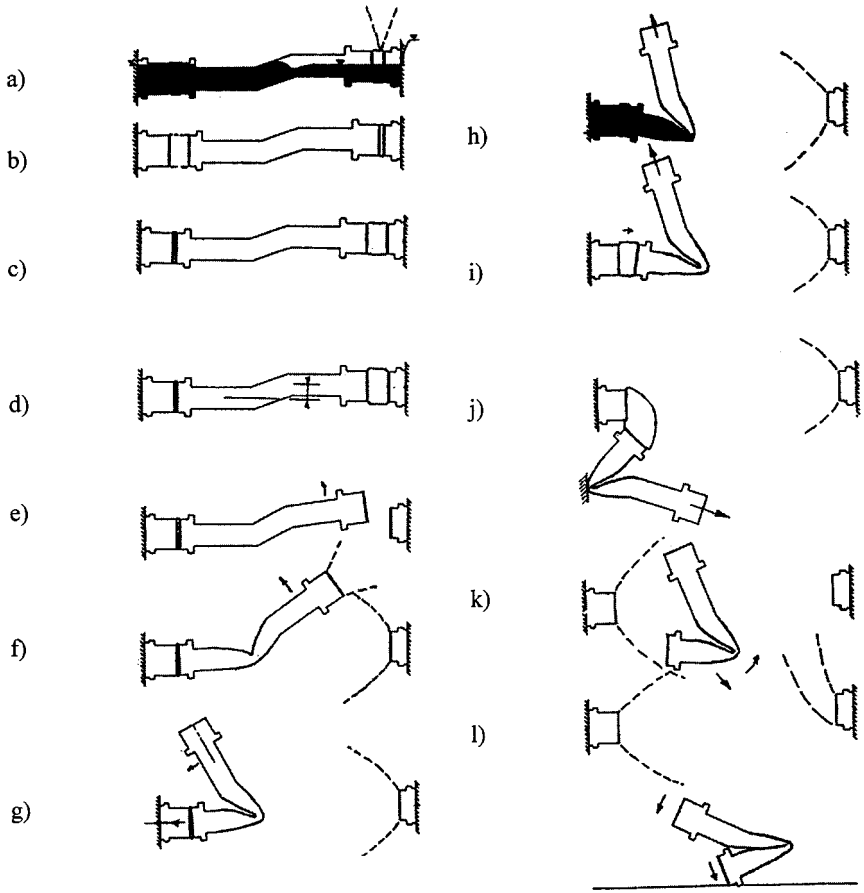

FIGURE 42.8 Successive stages of a crack-initiated two-stage bellows and pipe bridge failure.

only two months later *under* extensive debris between the line of reactors and the after-reactors (Foley and Nicholson, 1974); *all other portions of both the B4 and B6 bellows had been immediately located by investigators* (Foley, 1974a).

- The p-V work of the expanding two-phase supersaturated cyclohexane in the squirming and expanding B4 bellows, with the now greater constraint offered by the now compressed B6 bellows, buckles and completely collapses the 0.5-m pipe at its lower miter bend (Fig. 42.8*g*).
- The shape of the buckled pipe is now momentarily like the "swan neck" (Fig. 42.8*g*,*h*) noted by some (Marshall, 1974; Gugan, 1974b) with a significant vertical jet discharge. The B6 bellows through all of this is, however, still intact, though possibly severely damaged.
- In the process of suddenly buckling (Fig. 42.8*g*,*h*), the 250-kg liquid contents in the lower end of the 0.5-m diameter pipe are forcibly ejected into R6, and this impulse tears off its inlet baffle and causes this to impact and bend the internal 154-mm diameter SS agitator shaft (Artingstall, 1974; Gugan, 1978).

TABLE 42.1 Sights and Sounds in the Flixborough Bypass Pipe Bridge Failure (Fig. 42.8)

Time (s)	Event (Fig. 42.8)	Sound	Sight	Comment
1–2	(a)	PRV vent	Whisp to jet of "steam"	Many observers
3	(b)	"Thud"	Jets of "steam"	
3–4	(c)–(d)	Bang and rumble	Two-phase jet	
4+	(e)	Greater rumble, larger jet		Bellows squirms
5−	(f)–(g)	More severe rumbling	Upward debris, large kettle spout	Bellows off, pipe buckles
5	(h)–(i)	Roar "like a jet engine"	Vertical venting "swan-neck" pipe	Jet discharge, R4
5+	(j)	Pipe bangs R6	Vertical flames	Dent in R6
6–25	(j)	Continuing roar, first explosion	"Thrashing" jet flame	Jet discharge, R4, diminishes
26	(k)	Detonation	B6 tears off	R6 jet discharge
27+	(l)	Crash and thud	Buckled bypass impacts R5 plinth	R6 jet fire on B4 remnants and the 8-in. lines

- This process would have been very noisy because the bellows burst and the dog-leg pipe buckles sending the overhead scaffolding upwards. There would have additionally been the development of a roar due to the massive two-phase discharges from both R4 and the B4 end of the pinched pipe bridge and the rumbling of the boiling of the superheated Cyclohexane in R4 (Table 42.1).
- The choked two-phase discharge, which occurs through the B4 end of the pipe bridge via the 0.5-m pipe pinch—as the R6 internal pressure now expands B6 and frees its constraint (Fig. 42.8*h*) allows the reaction of the escaping two phase jet to bend and distort the bellows, forcibly expanding and stretching its topmost elements to their full extent (~1 m) so that the swinging pipe can sweep the scaffolding below (Fig. 42.3) toward the base of the R6 reactor (Plates 8 and 9 of Secretary of State for Employment, 1975). The position of the crimple points in B6 differs significantly from those in B4 (Foley and Nicholson, 1974) indicating a different distortion process for this bellows.
- In this operation the pipe deflects and the lower surface of the bend impacts the side of R6, denting it (Artingstall, 1974), flattening the bottom of the pipe after the lower miter bend farther (Foley, 1974a) (Fig. 42.8*j*), and effectively cutting off flow through the pinch. Additionally, the topmost portion of B6 is stretched out flat, without any convolutions being left, unlike the companion piece of B4, where some convolution creases were still intact (Foley, 1974b).
- In this dynamic process, the B6 bellows are now torn off and the rebound from the R6 impact *and* the impulse of the two-phase release from the now open R4 end of the pipe spins the assembly downwards (Fig. 42.8*k*) such that the R6 end flanges, impact the top of the 0.46-m-thick reinforced concrete R5 plinth, puncturing it (Secretary for State for Employment, 1975). The R6 stub end pipe and flanges are severely distorted at the point of impact by this process (Foley, 1974a).
- These later sequences (Fig. 42.8*h–k*) occur *after* the major explosion and explain the somewhat vertical but moving jet flame film taken by a witness (Goodchild, 1975) and observed earlier by others (Carter, 1974).

- Once the B6 bellows has blown off the resulting horizontal, northward developing torch flame envelopes the now blast damaged 8-in. pipes and causes the observed creep swelling and zinc contamination (Foley and Nicholson, 1974) of these as well as the high temperature carburization found *only* on the attached remnants of the B4 bellows of the R4 stub pipe (Foley, 1974a).

The major consequence of this sequence of events is that a discharge through reactor R4 *alone* occurs *prior to* the main explosion. This is sufficient only to provide a release of some 370 kg/s of cyclohexane for probably less than the 30 seconds determined for the initial events (Cox, 1976). This vent, of some 10–15 tons (Leclude 1996; Leclude and Venart, 1996), is very much smaller than the 30–60-ton estimates previously attributed to the explosion (Sadee et al., 1977; Roberts and Pritchard, 1982; Bjerketvedt et al., 1997).

Thus far, the postulated complex movements of the bellows-pipe assembly have been described such as might have occurred with a fatigue-initiated tear in the B4 bellows. The detailed finite-element analysis of the bellows and pipe bridge behavior supporting this interpretation is described next, and then the remainder of the section examines the discharge processes for the case postulated by the Court and that which would have resulted under the circumstances outlined above. We will thus compare the developments of the vapor cloud noted by witnesses and the consequences of its ignition.

42.4 FINITE-ELEMENT ANALYSES

The elastic lateral stiffness of a bellows decreases linearly with increasing pressure (EJMA, 1993; Newland, 1964; Snedden, 1985) and, upon sufficient increase, the bellows can become unstable, usually resulting in very rapid (10 to 50 ms) gross lateral deflection or ''squirm.'' The lateral stiffness and response of a universal expansion joint, i.e., two bellows interconnected by a straight length of pipe or spool piece, has been considered by Newland (1964). The lateral stiffness for two bellows connected by an offset spool piece, such as here, was undertaken by Newland (1976). No determination appears to exist for the determination of natural frequency with an offset spool piece.

ANSYS 5.3 (Swanson Analysis, 1994) nonlinear elastic-plastic large deformation finite-element (FE) models were made of the bellows and assembly illustrated in Fig. 42.8. The bellows and 0.71-m OD stub pipes were fabricated from 316L SS; the 0.508-m OD dogleg pipe bridge was made from four sections of 4.8-mm-thick 304L SS pipe with two 80° miter bends (Foley, 1974a).

42.4.1 The Bellows

The bellows (Fig. 42.9*a*) was originally formed from 1.19-mm-thick sheet. In the forming process, the thickness was reduced to 1 mm, (t) and the material cold worked. Each bellows had 12 convolutions (N) and was about 230 mm long overall with a 750-mm mean diameter (R_m = 375 mm, t = 1 mm, p = 33.9 mm, h = 37 mm).

The mechanical properties used in the models were determined from samples cut (in both longitudinal and transverse rolling directions) from a 1.2 by 2.4-m 316L sheet 1.19 mm thick. Mechanical properties were also determined after a single-pass cold-roll reduction to 1 mm. Twenty samples (five for each direction, both as received and single pass cold rolled) were utilized. The mean results are given in Table 42.2. Directional variation was between 2.6 and 3.4 and 4.8 and 6.7% on strength for the as-received and cold-rolled specimens respectively.[3]

[3] ASTM subsize sheet type E 8M 89b specimens; Instron servohydraulic testing machine, load cell in series with the specimen.

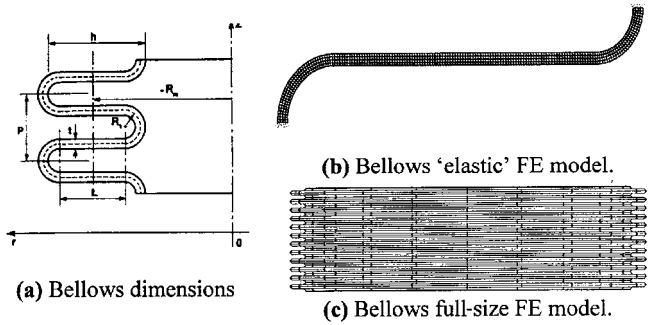

FIGURE 42.9 Bellows dimensions and models. (*Source: Venart and Tan, 2000.*)

For small deflections (i.e., elastic behavior), a bellows can be simplified by only half a convolution (Fig. 42.9*b*). The axial and transverse stiffness from such an analysis can be regarded as a reference base for the verification of any later more detailed, and therefore necessarily less refined, FE model. An analysis using 2688 eight-node isoparametric 2D symmetric elements, PLANE82, with 8753 nodes, resulted in a determined axial stiffness, K_{axial} of 403.8 kN/m (2,306 lbf/in) with a transverse stiffness, $K_{\text{transverse}}$ of 5,558 kN/m (31,738 lb_f/in.). Experimental values obtained from the manufacturer (Batstone, 1975) were stated to be between 485 and 578 kN/m and 7,567 and 9,015 kN/m for the axial and transverse directions respectively. The differences could be due to nonisotropy due to the forming process and the choice of a uniform wall thickness in the model.

With large transverse deflections, contacts between adjacent convolutions occur and the whole bellows must be modeled. The shape of the bellows is asymmetric, i.e., the overall shape of the deformed structure possesses 180° rotational symmetry about the midpoint of the neutral axis. Three-dimensional shell elements (SHELL43) are thus necessary (Fig. 42.9*c*). An element size of 12 × 12 mm yields 11,760 elements and 11,979 nodes to mesh only one half a bellows. The computational requirements for this are large. Increases in element size result in an increase in axial stiffness.

Figure 42.10 illustrates the relative transverse deflection of the present model as element numbers are increased. When the sum of elements exceeds between 500–650 a near asymptote is reached. A maximum element size of 125 mm was therefore chosen using 720 elements with 803 nodes to model the bellows (Fig. 42.9*c*).

Figure 42.11*a* shows the deformed shape of the bellows joint with an axial extension of 5 mm at an internal pressure of 0.96 MPa and a transverse displacement of 75 mm. Figure 42.11*b* shows the transverse loads required to effect the displacement as a function of internal pressure (0.1 and 0.96 MPa). Four main stages can be observed. The first stage, stage I, is the linear elastic range; here the load-deflection curve is linear and the stress in the bellows is below the yield strength. The second stage, II, is a primary yielding range; localized

TABLE 42.2 Mean Mechanical Properties for As-Received and Cold-Rolled 316L SS Sheet

	Yield strength s_y MPa (kpsi)	Ultimate strength s_u MPa (kpsi)	Elongation (%)
Bulk	275 (39.9)	607 (88.0)	55
Cold rolled	648 (93.9)	766 (111.0)	37.2

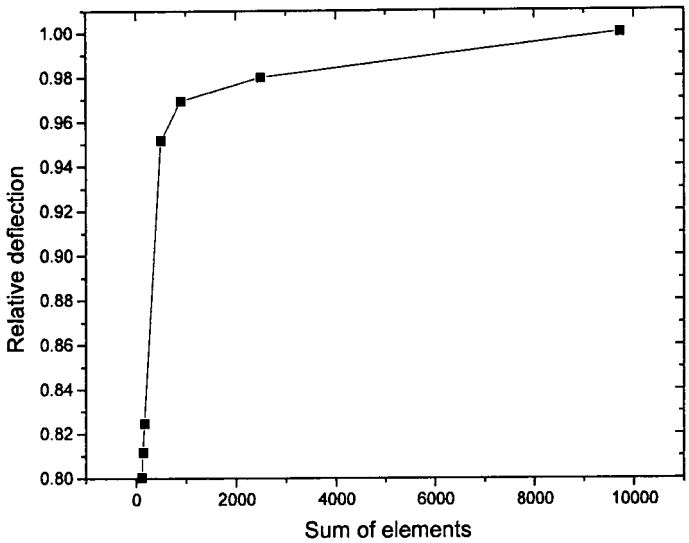

FIGURE 42.10 Total element numbers versus relative transverse deflection (stiffness).

yielding occurs at the tops or bottoms of the convolutions where stress levels are high. With increased loading, the bellows go into a third stage, III, where contact between convolutions occurs. This stiffens the bellows in the lateral direction and so the slope of load-deflection curve increases. The final stage, IV, is of general plastic deformation where the whole bellows yields and the slope of the load-deflection curve decreases until final rupture.

Snedden (1985) experimentally obtained similar load-deflection curves and developed simplified analyses to determine the collapse pressure and evaluate the first three ranges noted above. He considered the lateral stiffness once convolution contact occurred to be infinite and thus any constraint to be rigid, though as can be seen from his results, this is far from the case (Fig. 7 of Snedden, 1985) and a more gradual approach to failure develops.

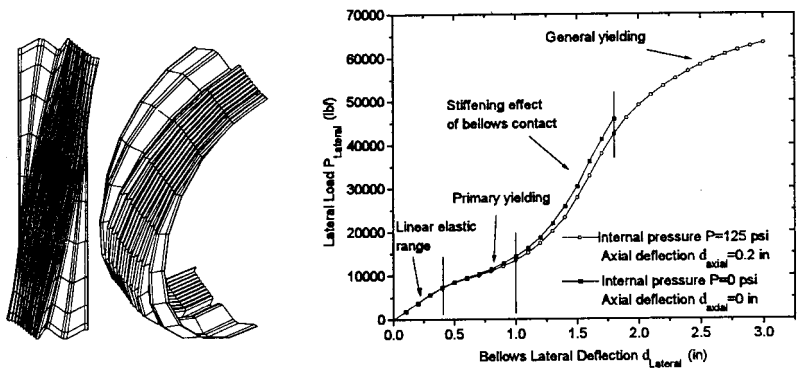

(a) (b)

FIGURE 42.11 Large-scale deformation of bellows: (*a*) with imposed axial deflection under internal pressure and lateral loading; (*b*) load in lb_f, pressures in psig, deflections in inches.

The limiting internal design pressures, based on column instability (both ends rigidly supported) and no axial extension, are estimated by EJMA (1993) methods to be 2.1 MPa (290 psig) and 1.8 MPa (246 psig) for the cold and hot bellows respectively.

42.4.2 The Bellows and Stub Pipes

Batstone (1975) conducted four individual water-filled bellows tests with a facility designed to simulate half the dogleg pipe/double bellows assembly (Fig. 42.12). Because the distance from the midpoint between the two miter bends to the first convolution of each bellows differed by only 17.5 mm, only the lower, R6, bellows was evaluated. Axial and shear forces on the bellows were measured as functions of internal pressure along with vertical deflection measurements. The pivot point of the pipe assembly was fixed 0.178 m above the centerline of the bellows at zero internal pressure at a distance of 2.4 m to the first convolution. The ends of the bellows were welded to stub pipes and these bolted to blank flanges, the fixed end being bolted to the support frame and the free end being welded to an I-beam that supported the pivot point of the assembly.

The bellows all failed, i.e., squirmed, at an internal pressure of about 1.2 MPa. In one of the tests, pressures were cycled over selected ranges of up to 3,456 times. In this test, cracks did not occur until further pressurization to 1.5 MPa. These cracks were sealed and the test cycles continued for 900 cycles (1.0 to 1.1 MPa) and a further 400 cycles (1.07 to 1.2 MPa); there was only a slight increase (2 mm) in the three cracks that had formed at the crimple points due to squirm. In a few experiments a 48-mm-diameter 1.82-m-long scaffold support was provided with a 6.4-mm space between stub pipe flange in order to evaluate the influence these had on the behavior.

The large deformation FE model for these experiments was set according to Fig. 42.13. The bellows and stub pipe were simulated with 654 3-D 4-node elastic-plastic shell elements (bellows 514, pipe 140 elements). The stub pipe flanges were simulated by different thicknesses in order to maintain appropriate gravity loading with the fluid contents. The linkage between the flange and pivot was simulated by a group of very stiff beam elements.

Internal pressure in the model was increased gradually and both the axial and vertical loads at the pivot as well as the vertical deflections of the bellows were computed. A beam element and a contact element, with a set gap of 6.4 mm, could be used to simulate the scaffold support.

A comparison between measured and simulated loads in both the axial and vertical directions shows that these were similar. Figure 42.14 indicates the vertical deflections as a function of internal pressure. Although there are some differences, agreement is reasonable,

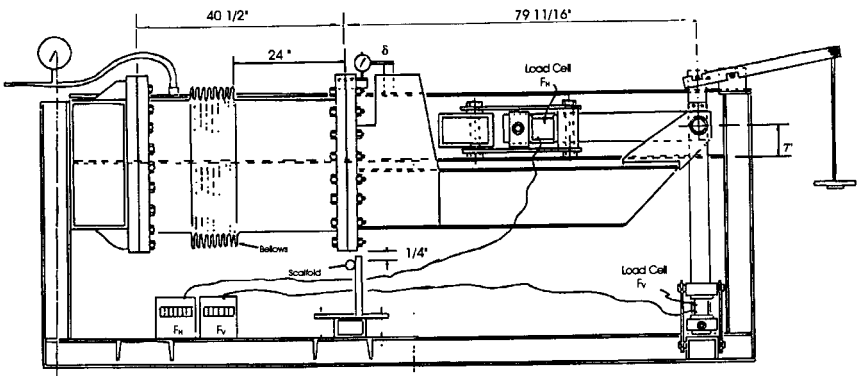

FIGURE 42.12 Bellows test facility, dimensions in inches. (*Source: Batstone, 1975.*)

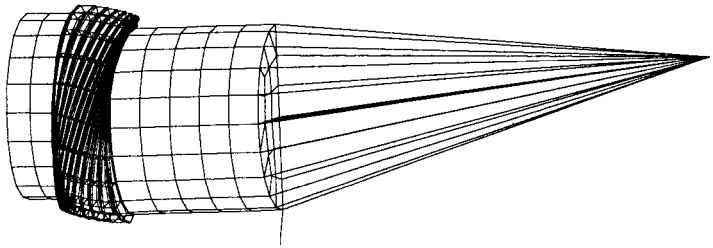

FIGURE 42.13 Finite-element model of the bellows test.

with the FE model generally more compliant. One possible reason for this is that the bellows used in the experiment had been cycled extensively with pressure, which could cause a certain degree of strain-hardening before the final cycle loading when the bellows squirmed. The final measured and simulated squirming pressures are, however, very nearly the same (1.24 MPa).

42.4.3 The Bridging Pipe

Experiments on the 4.8-mm-thick wall dogleg pipe were also carried out (Batstone, 1975) (Fig. 42.15). Two 75-mm pin joints were located at the center of the bellows at each end of the original assembly, where the bending moment was zero. An axial load was applied horizontally at the lower end through two precalibrated hydraulic rams, each of 100 ton capacity with 152-mm stroke. In order to support the vertical force on the ram, two double-row, self-aligning ball bearings were located on the extended pin of the joints. These were

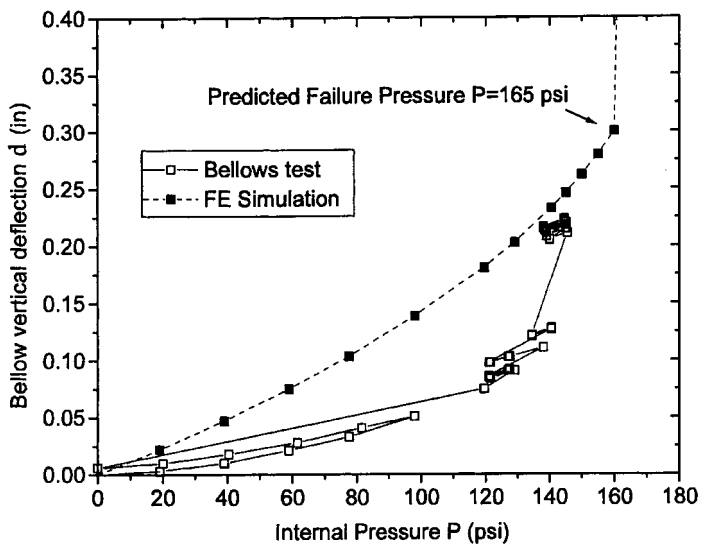

FIGURE 42.14 Bellows vertical deflection as a function of pressure; test, Batstone (1975) and FE simulation, pressure in psig, deflection in inches.

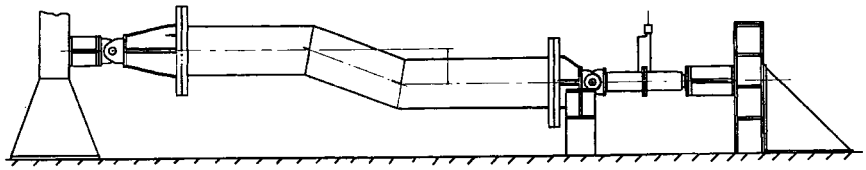

FIGURE 42.15 Bypass pipe experimental facility. (*Source: Batstone, 1975.*)

free to move on two horizontal supports mounted on the floor as the rams extended but were prevented from twisting. Two strengthened adapter pieces were welded to blank flanges bolted to both ends of the pipe and pivoted on pin joints fixed to vertical support columns. The pipe itself was filled with water and internal pressure applied with a hand pump. The axial load applied via the ram maintained the internal pressure according to the relationship:

$$F = PA \tag{42.1}$$

where F was the horizontally applied axial load, P the internal pressure, and A the effective cross-sectional area of bellows ($d_{\text{eff}} = 747$ mm). The internal pressure and deflections at several positions were measured and recorded.

The FE simulation of this test was simpler than that for the earlier bellows model. The pipe was represented with shell elements (SHELL43) and the strengthened adapter pieces, which connected the blank flanges and the pin joints, were represented by beam elements as shown in Fig. 42.16. The weights of the two heavy flanges, each with 28 bolts, nuts, and washers, the adapters, and the water-filled pipe were converted into equivalent thickness of shell and beam elements similar to that in the bellows simulation. Internal pressure and axial forces were applied to the pipe instantaneously.

A comparison of the model results to those of the experiments shows that the test data exhibit a greater yield load in addition to a prestrain (Fig. 42.17). This might have occurred because a previous load, beyond yield, was experienced in earlier testing of the pipe used (Games and Waterhouse, 1974). The measured load-deflection curve, shifted by 7.6-mm, post yield, appears to correspond well to the FE simulation; both indicate a final failure by buckling at an internal pressure of about 1.93 MPa (265 psig).

In order to evaluate the influence of end constraint on pipe behavior, a further FE study was conducted using this model. This employed a ''hard'' or fixed constraint at the B6 end that restricted rotation of the pipe and thus simulated the compression of the B6 bellows corresponding to the stage III bellows model of Snedden (1985). This showed that an internal pressure of only 0.76 MPa (95 psig) caused buckling failure of the pipe at its lower miter bend. Relaxing the B6 constraint would obviously increase the buckling pressure. Such a result indicates that, had a differential pressure occurred across the two reactors, such as could have happened by only one bellows suddenly tearing and depressurizing, squirm of that bellows *and* buckling of the pipe assembly was possible at operating pressure (Venart, 1999).

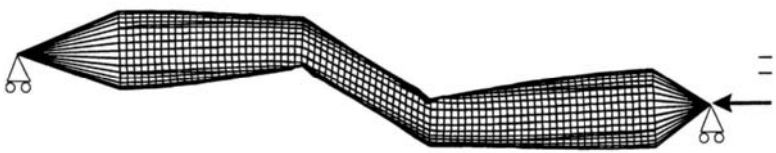

FIGURE 42.16 FE model of bridging pipe. (*Source: Venart and Tan, 2000.*)

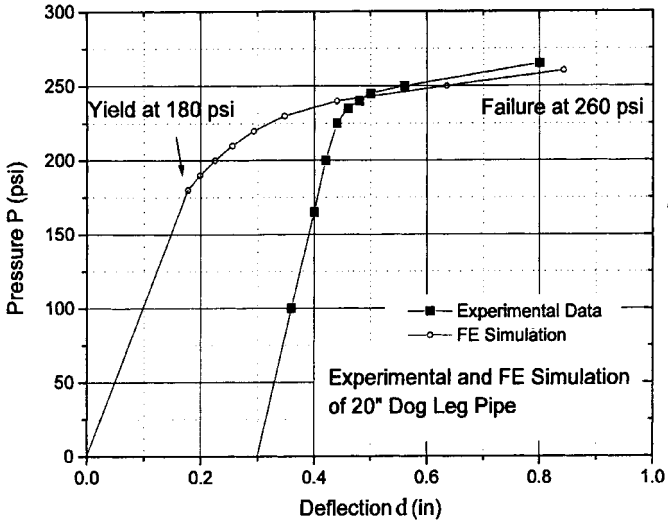

FIGURE 42.17 Load deflection of the bypass pipe; experiment (Batstone, 1975) and FE model, pressure psig, deflection in inches. (*Source: Venart and Tan, 2000.*)

42.4.4 The Bridging Pipe–Bellows Assembly

Both static and dynamic FE analyses for the assembly were made based on the previous models. The model setup, loads, and weight conversions were similar to those used earlier. The main difference was that the pipe was not fully filled with cyclohexane (Teng-yang et al., 2000; Venart, 1999) and that a scaffold system could be set to support the pipe assembly (Figs. 42.4 and 42.18).

The Experiments. A test of the assembly was conducted at Flixborough using a new pipe built according to the original design and inserted in place of reactor 3 (R3) (Secretary of State for Employment, 1975; Games and Waterhouse, 1974). The bellows utilized were new, with axial stiffness of 498 (2841) and 482 kN/m (2753 lbf/in) for the B4 and B6 bellows respectively. Scaffolding similar to that in the original installation could also be used. Axial and lateral deflections were measured, both cold and hot (155 and 160°C), with a chain used to simulate the dead load of the fluid inventory. Pressure was applied by nitrogen gas. Strains in the pipe were also measured. There were eight test runs, three at ambient temperature, three at 155°C, and two at 160°C. The maximum pressure utilized was 0.964 MPa in all but

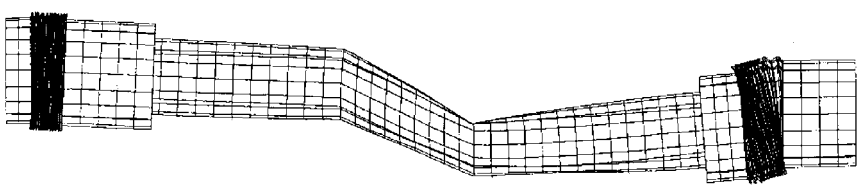

FIGURE 42.18 FE model of the Flixborough bypass assembly at an internal pressure of 0.964 MPa (125 psig); deformation scale exaggeration is 100. (*Source: Venart and Tan, 2000.*)

the last two cases; for these the bellows were squirmed at 1.06 MPa and then burst at 1.53 MPa.

In the experiments at ambient temperature, internal pressure causes the B4 end of pipe to move upward and the scaffolds there are only lightly loaded. With increase in pressure, the B4 end rises off the scaffold support as the B6 end moves downwards and the scaffolds there carry greater load. However, under operating conditions, 150 to 155°C, the assembly was mostly unsupported since the reactors expand upwards about 6 mm. The scaffold supports are thus neglected in the FE analysis under operating conditions, though they were needed to commence the analysis.

***The FE Model* (*Fig. 42.18*).** Four load steps were used in the FE simulation of the complete assembly:

1. The by-pass pipe rested on the scaffolding without internal pressure.
2. The system was next pressurized.
3. The assembly was set free due to the upward thermal expansion of the reactors (6.4 mm).
4. The pipe was allowed to thermally expand axially (approximately 10 mm) along with the radial expansion of each reactor and its stub pipe (about 2.5 mm). At the lower or R6 end contact and deformation of the scaffolding was permitted if the downward assembly deflection exceeded 6.4 mm.

In the model it was assumed that the upper pipe was half full and the lower pipe full of liquid cyclohexane. It was also assumed that the scaffolds were made of normal structural steel; these were simulated by beam elements with contact elements to prevent any loading when the pipe contact was lost. Elastic-plastic load-deflection relationships were used to simulate the pipe, the bellows, and the scaffolding.

The vertical deflections at the two ends of the pipe, obtained for an internal pressure of 0.964 MPa, are listed in Table 42.3. Compared to the experimental measurements, the trends are similar. However, there are some differences in the values, particularly for the upper bellows where the experimental deflections exceed the FE results by some 35%.

TABLE 42.3 FE Analysis of the Assembly and Comparison with Test Data[a] Vertical Deflections[b]

Case	Condition	Deflection at upper, B4, end of pipe, mm (in)	Deflection at lower, B6, end of pipe, mm (in)
FE initial (a)	Full scaffold support no internal pressure	−0.72 (−0.028)[c]	−0.77 (−0.030)
FE at 20°C (b)	Partial scaffold	3.41 (0.134)	−3.77 (−0.148)
FE at 150°C (c)	Partial scaffold support, 0.964 MPa	6.93 (0.273)	−4.49 (−0.177)
(a)–(b) FE Cold	Scaffold support, 0.964 MPa, Cold	4.13 (0.163) [10.66 (0.4195)][d]	−3.00 (−0.118) [−3.26 (−0.1285)]
(a)–(c) FE Hot	Partial scaffold support, 0.964 MPa	7.65 (0.301) [10.27 (0.4042)]	−3.72 (−0.147) [−3.26 (−0.1285)]

[a] Games and Waterhouse, 1974.
[b] Venart and Tan, 2000.
[c] + upwards, − downwards displacement.
[d] Average values from experiment, Games and Waterhouse, 1974.

The maximum von Mises stresses, 231 MPa (33.5 kpsi), occur along the tops and bottoms of the convolutions, particularly at the second-to-last convolutions of both ends at normal operating conditions. One of the regions is apparently coincident with parts of the internal tear noted by the Court (Secretary of State for Employment, 1975; Foley, 1974a) (Fig. 42.19). Stress levels in the lower bellows are similar to those in the upper bellows. The stresses in the experimental bellows at B4 would, however, have exceeded these values since deflections were larger.

At temperature and pressure, the upper (R4) end of the pipe moves towards R2524 by 0.67 mm; the absolute axial displacement of the other end of the bellows is away from R2524 by 2.89 mm, so that the axial compression of the upper bellows is 3.55 mm. At the lower (R6) end of the pipe the assembly moves away from R2526 by 0.037 mm with the absolute axial displacement of other end of the bellows moving away from R2526 by 3.08 mm; the axial compression of this bellows (B6) is thus 3.05 mm. The pipe, between bellows, shortens under these conditions by 3.51 mm compared to a measured value of between 5 and 7 mm (Games and Waterhouse, 1974).

FE Modal Analysis of the Bypass Pipe Assembly. In the pipe model previously described, the mass of fluid was converted into a density increase as a function of location. The total weight of the pipe, flanges, bolts, bellows, and insulation was about 1.13 tons and its liquid inventory some 600 kg, of which at least 375 kg were distributed in the lower half of the pipe under operating conditions.

The first three natural frequencies and vibration modes were determined using modal analysis. The first natural axial frequency was found to be $f_1 = 3.98$ Hz. The second natural, and transverse (vertical) frequency (coupled with bending of the pipe) was $f_2 = 12.35$ Hz. The third natural frequency was $f_3 = 30.16$ Hz; this mode of vibration was the rocking mode of the assembly. The equivalent determinations based on EJMA (1993) are 3.93, 15.7, and 27.2 Hz respectively. The axial mode agrees well, but the inclusion of the offset pipe appears to reduce the transverse and increase the rocking modes.

Three main harmonic forces are induced with the flow system (Teng-yang et al., 2000). One is the axial load that results from the flow fluctuations at the diameter change in the

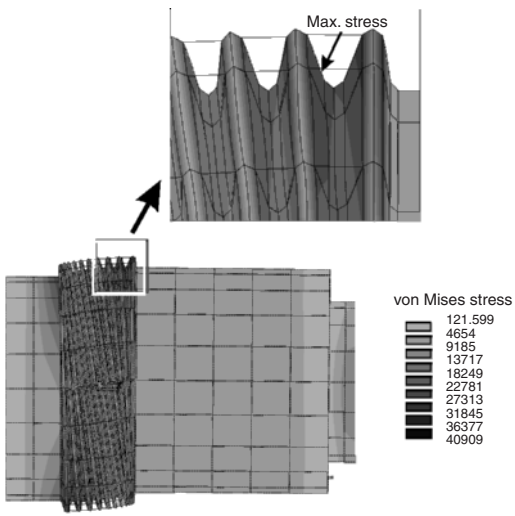

FIGURE 42.19 Static equivalent (von Mises) stress upper B4 bellows, stress in psi.

TABLE 42.4 The Harmonic Response of Bypass Assembly as a Function of Frequency

Frequency f (Hz)	1.15	1.52	1.89	2.26	2.44
Response Amplitude: s_{eq}; MPa (psi)	31.1(4514)	31.5(4570)	31.9(4626)	32.3(4682)	32.5(4710)

upstream pipe. Another is the transverse loading due to the change in fluid mass at the lower hydraulic jump. Both these forces are in phase and at the same frequency as the hydraulic head change. Due to the hydraulic jump after the upper miter bend the mass, in the lower half of the pipe would have oscillated by about 60 kg (~3.5% of the total system mass) at a frequency of between 1 and 2.5 Hz. A third force is the level fluctuation in the weir waterfall pools; levels in similar-sized outfalls vary with a frequency of about 7 Hz (Rajaratnam and Chamani, 1995). Further, the plunge pool jet velocity, even for the lowest flows, is sufficient to excite axial resonance of the bellows as noted earlier.

The lowest natural frequency of the system was earlier determined to be about 4 Hz. Since the frequency of driving excitation is 50% of the lowest natural frequency, a simple sensitivity analysis was performed in order to determine its influence. It was found that as the driving frequency increased from 1.15 Hz to 2.44 Hz, the harmonic response increased only 5%. The results are listed in Table 42.4.

Damping is important in any harmonic analysis. Due to the complexity of this fluid-structure interaction problem, the damping of the system was difficult to determine and an approximation was made based on a sensitivity analysis. First damping is very low for stainless steel; values of 10^{-3} to 10^{-5} are normally assumed; damping in gas or vapor spaces would likewise be small, i.e., the top of B4. For the liquid-structure coupled portion of the system, damping could be large (e.g. B6 and the bottom half of B4) and was therefore assumed to be 0.5. An analysis within this range is illustrated in Table 42.5, which indicates that the amplitude of the equivalent stress is quite stable for damping coefficients in the range of 0.001 to 0.3.

The comparison between the finite-element models and the experiments undertaken above indicate that the models reasonably represent the behavior of the bellows, bellows and stub pipes, as well as the bridging pipe. The interpretation of how the assembly could have behaved with a failure in the B4 bellows follows closely that shown in Fig. 42.8, discussed earlier.

42.4.5 Summary of the Finite-Element Analyses

Finite-element models of the Flixborough bellows, bellows and stub pipe, bypass pipe, and the complete bypass assembly have been made. The analyses permit the following conclusions:

TABLE 42.5 Harmonic Response of Bypass Assembly with Damping Coefficient ζ

Damping coefficient ζ	0.001	0.01	0.1	0.3	0.5
Response amplitude: s_{eq}; MPa (psi)	31.1(4509)	31.1(4509)	31.0(4486)	29.7(4315)	25.9(3761)

- The FE model of bellows under large lateral deflection reasonably replicates the experimental behavior observed by Batstone, Snedden, and others.
- The model of the bellows and stub pipe assembly behaves in a similar manner to that in the experiments; failure, that is, squirm, occurs at similar internal pressures.
- The model of the bridging pipe corresponds well to the experimental behavior of the pipe with the imposed end constraints; with increased end constraint at the lower, B6, end of the pipe, the structure can buckle at a considerably lower pressure.
- The deflections of the complete bypass assembly model replicate the trends of the experimental data obtained by Games and Waterhouse for both the ambient and hot experiments. The maximum von Mises stresses occur along the topmost bellows elements. Some of these points appear to coincide with the locations of portions of the internal tear found in one of the recovered B4 bellows pieces.
- Modal analysis of the complete bypass assembly indicates that excitation by the flows was possible, and a harmonic response analysis, considering the possibilities of damping, indicates that some greater concern for fatigue failure should have been considered.
- A possible failure mechanism for the bypass pipe assembly that only involved the release from the upstream, R4, reactor has been indicated.

42.4.6 The CFD Analyses

A transient three-dimensional CFD model was developed for a 130 (x) by 130 (z) by 30 (y, elevation) m volume shown in Fig. 42.2 (Venart, 1999). The region considered encompassed the reactors and after-reactor vessels and their plumbing (especially the 8-in. lines) in Sections 25A and 7 (and a portion of Section 27), the laboratory, and the control room, as well as the main and works office buildings.

The time marching computations were carried out using the commercial code ***FloSYS*** (Flomerics, 1994), which is a CFD solver operating in Cartesian coordinates.

The solution was performed throughout the rectangular cuboid domain for the velocities u, v, w in the x, y, and z directions respectively, fluid static pressure, p, temperature, T in the gas and solid regions, and concentration of the secondary medium (Cyclohexane), c. Several tests were evaluated for solution convergence, and as a compromise among accuracy, computational requirements, and resources, a grid system of $98 \times 41 \times 68$ nodal points in the x, y, and z directions respectively was selected. The smallest cell size, commensurate with the smallest scale of detail, the 8-in. pipe, was 0.1 m in the x and z directions and 0.05 m in the y direction; the largest cell sizes were on the upper domain corners; these were typically $3 \times 2.3 \times 3.3$ m in the x, y, and z directions, respectively. The grid, where required, was set automatically to reconcile with internal solid surfaces particularly in the reactor near field.

The equations solved formulate the principles of conservation of mass, momentum in the x, y, and z directions, thermal energy, and mass of secondary medium (cyclohexane). Turbulence modeling is performed by using a standard two-equation (k-e) turbulence model with near-wall grid node wall functions used to evaluate surface friction and surface heat transfer. The effects of turbulence are represented via a turbulent viscosity and thermal diffusivity where these quantities are linked by the turbulent Prandtl number, which takes a constant value of 0.9.

Buoyancy effects due to thermal expansion and the heavy vapor dispersion of the evaporated cyclohexane are included in the y direction as a gravitational source term. The variation of properties, in this particular case, density, is assumed to be governed by the ideal gas laws. The molecular viscosity, thermal conductivity, and diffusivity were taken to be those for air and constant.

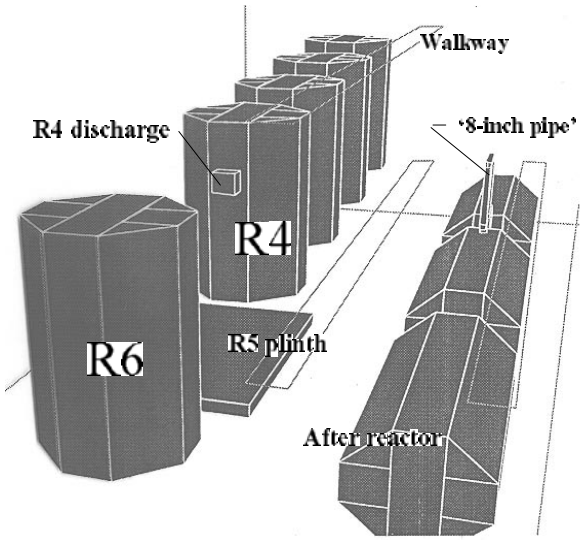

FIGURE 42.20 A near-field northwest view of the reactor train and the after-reactors as might have been seen from the roof of the main office building. (*Source: Venart, 1999.*)

Plant equipment, pipe racks, and supporting structures, other than the five reactors and the associated after vessels and plumbing, were treated as flow obstacles with a uniform resistance and porosity of 0.5. Buildings and other large structures (the main office, the works office, the laboratory, and the control room) were assumed to be impervious to the flow and adiabatic. The prevailing wind was assigned by steady vector components as boundary conditions on the free boundaries of the domain. The surface of the ground was set to a uniform roughness of 0.01 m.

The mass source terms, representing the flashing two-phase discharges from the reactors, were evaluated from prior choked flow determinations and the assumption of sonic, vapor-only flow at the reactor, R4 and R6, outlet nozzles (Leclude and Venart, 1996). The properties of cyclohexane and its dissolved nitrogen were obtained from the NIST (1990) mixture property program, STRAPP.

A near-field isometric view of the reactor train is shown in Fig. 42.20 as represented in the Flomerics code. In the figure, the walkways along the reactor train are represented by porous resistance areas, and the 8-in. pipes connecting the two after-vessels together are indicated. The cuboid representations of the vessels are also shown.

The FloSYS ASCI output files were used as input files to be further processed by Tecplot (Amtec Engineering Inc., 1996) to extract the isocontours for the lower (LFL) and upper (UFL) flammable limit (0.037 and 0.198 wt. % respectively) and determine interactive visualization through time-sequenced plots of the isosurfaces.

42.4.7 CFD Results

Simulations were preformed for two cases: (1) the simultaneous discharge from both R4 and R6, as the base case representing that process accepted by the Court, and (2) a discharge from only R4 prior to the explosion, as the situation explored here. In both instances the

discharges were taken as choked sonic cyclohexane vapor at 370 kg/s and 150°C. The results are available in the form of movies[4] or animations both for the far-field and close-in regions of the computational domain.

The transient development of the Cyclohexane vapor cloud at its lower and upper flammable limits (LFL and UFL respectively) over a period of 30 seconds will be shown as a Tecplot movie. The UFL is represented as the paneled interior surface, and that for the LFL, the wire-frame exterior surface in the figures which follow.

***Discharge from Both R4 and R6* (*Fig. 42.21, Movie 1*).** The first frame illustrates the computational domain, as indicated in Fig. 42.2, to a height of 30 m, showing the placement of portions of the laboratory, the main control room, the main office and the works office. The reactor train is indicated along with the after-reactor and treatment vessels in addition to the 8-in. lines. Also included are the access walkways along the reactor train and the rest of plant, approximated as porous areas and volumes respectively, both with porosities and resistance coefficients set to 0.5 as estimated from the site photographs in the Report of the Inquiry and other sources. These areas are indicated as transparent boxes or areas outlined in color.

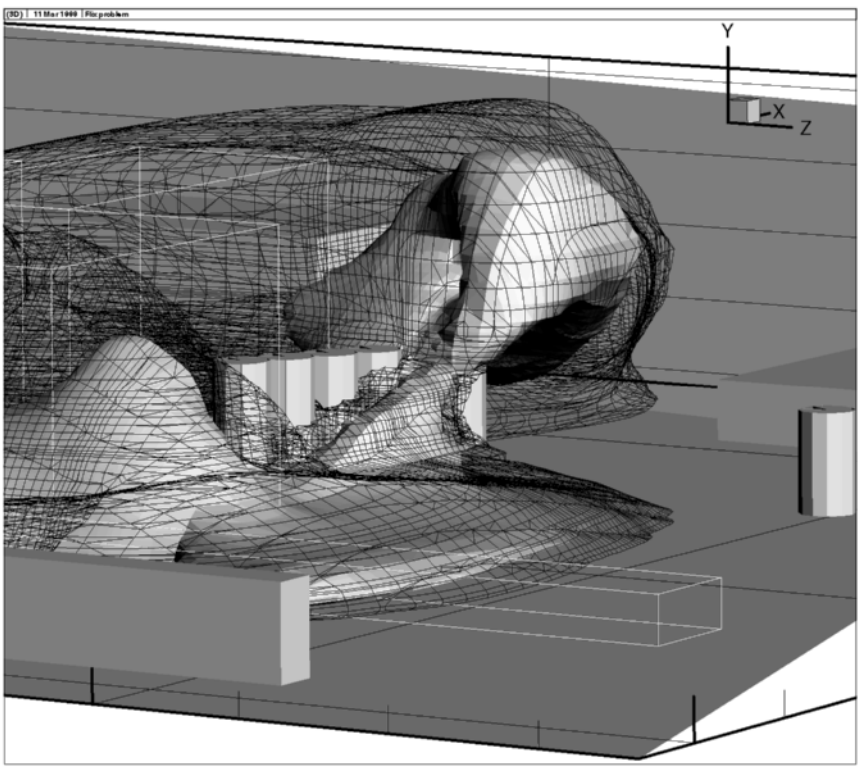

FIGURE 42.21 Southeast view from the top of the hydrogen plant looking towards the main office building: R6 and R4 discharges at 12 seconds, LFL and UFL envelopes. (*Source: Venart, 1999.*)

[4] The movies are available from the author and may be played using a supplied utility.

The sequence of all frames is at one-second intervals.

It can be seen that the simultaneous discharges, even at one second into the event, result in an aerial cloud from the discharge of R4, riding up and over both the jet discharge from R6 and the top of this vessel and reaching to a height of about 20 m. This cloud proceeds southerly into the prevailing wind and towards the opening between the two office blocks.

At the same time, the R6 discharge is split by R4 into two jets and channeled by the R4 jet above, the reactor train walkways, and the after-reactor and reactor vessels to form a dense gas cloud moving predominately at ground level along the reactor train in a NNW direction.

After only two seconds, the LFL of this cloud has reached the northern end of the reactor train, i.e., R1; there is relatively little westward development of this cloud due to the intense momentum of the R6 discharge split by the R4 reactor.

At 8 seconds, the R4 cloud is still airborne (~24 m elevation at the LFL) and much larger and starting to slump towards the ground in a southerly direction with the LFL, making a footprint around the northwest corner of the main office building and commencing to exit from the domain in a southerly direction between the two buildings; the cloud does not, however, contact the works office. The R6 cloud, though now shown to have developed its LFL envelope up to some 16 m elevation, is, at its north-northwest ground boundary, approaching the laboratory with little westerly development. The height of this cloud would no doubt have been restricted by the floors in the rest of the open plant structure of section 25A and so the 16 m vertical extent of the LFL is perhaps an artifact induced by the use of uniform porosity and resistance.

By 12 seconds, part of the R4 UFL envelope has touched down between the office buildings and the LFL cloud has proceeded out into the car park at a mean velocity of some 4 m/s. The other portion of the R4 LFL cloud has exited to the east from the space between the north face of the three-story main office building and the southern end of sections 25 and 7. The R6 LFL envelope by this time has started to surmount the two-story laboratory building and is commencing contact with the control room; the westerly spread of the LFL has reached the westernmost end of the laboratory.

After 18 seconds, the R6 UFL envelope has reached the control room and has topped the two-story laboratory building. Both the LFL and UFL envelopes have exited from the western boundary of the domain towards the hydrogen plant. The R4 discharge LFL cloud continues to exit between the main office block and the southerly ends of sections 25 and 7 as well as southerly between the space with the works office; the UFL of this envelope has now mounted the northwest corner of the office block.

By 22 seconds, the R6 LFL and UFL envelopes have both surmounted the laboratory and the control room and are proceeding across the western domain boundary towards the hydrogen plant. The center of gravity of the main body of this cloud is situated just north of R1. Both the LFL and UFL R4 envelopes are now exiting from the southern domain boundary between the two offices and into the car park; the eastward LFL cloud still exits from the eastern boundary in the space between the main office and the southern end of section 7.

At 30 s, the R6 discharge clouds have proceeded northerly past the control room and laboratory. The R4 discharge cloud is still split by the main office block into two sections; one exiting into the car park, the other to the east between the office and the southern ends of sections 25A and 7.

***Single Discharge from R4* (*Fig. 42.22, Movie 2*).** The transient development of this vapor cloud differs significantly from that above. At the commencement of the event, a series of choked vapor discharges from a slit, set to be approximately similar to that noted in a piece of the B4 bellows by Foley (1974a), are shown for 0.2-second intervals up to 1 second followed by 1-second snapshots thereafter.

The first four frames portray the discharge from the slit in the R4 bellows as a westward-proceeding jet developing over a time span of 1 second. The next sequences show the

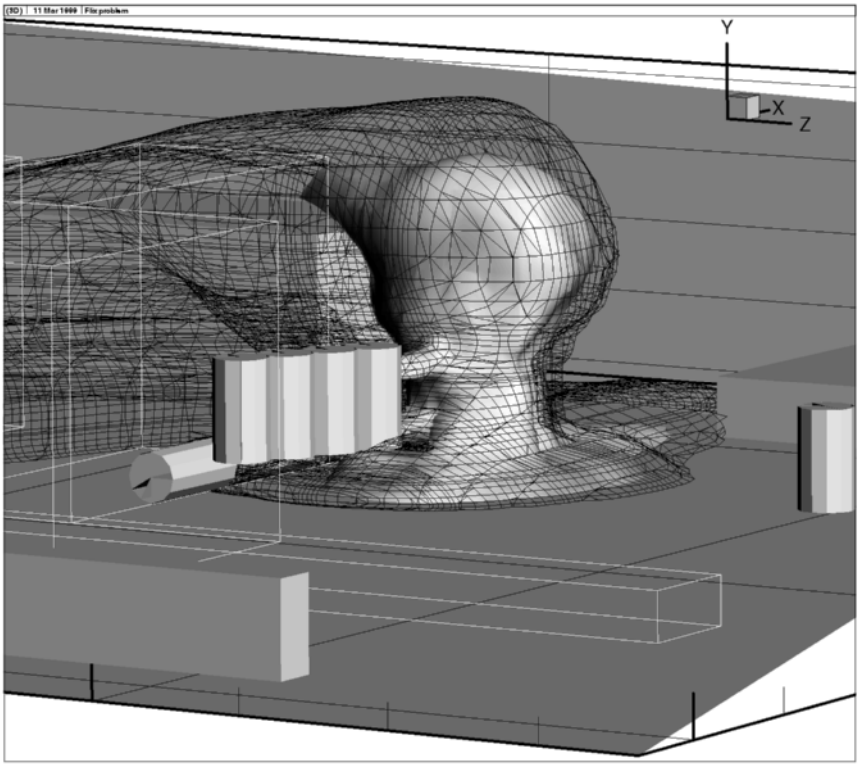

FIGURE 42.22 Southeast view from the top of the hydrogen plant looking towards the main office building: R4 discharge only at 12 seconds, LFL and UFL envelopes. (*Source: Venart, 1999.*)

interaction of the jet impact from R4 as it hits R6, when the B4 bellows is blown off and the jet formed is deflected upwards. By 4 seconds, the shape of both the LFL and UFL envelopes are roughly cylindrical; the height of the LFL cloud is about 25 m high with a cylindrical ground footprint of some 30 m diameter for the LFL and 15 m for the UFL.

At 6 seconds, the prevailing wind is distorting the LFL envelope; both the UFL and LFL footprints commence a westward progression across the open space in front of the works office and northward to the base of the R2 reactor (LFL). The LFL southern envelope approaches the NW corner of the Main Office building.

In 8 seconds, the LFL envelope's SE extremity has impacted the northwest corner of the Main Office building and has commenced exiting from the eastern domain boundary between the southern ends of section 25A and 7 and the northern wall of the office building. The base of the LFL footprint has progressed northward to the base of R1 with the northern boundary of the UFL just past the base of R4.

At 12 seconds, the momentum of the jet has pushed the UFL envelope to the northwest corner of the office building. The LFL envelope in its eastern branch is now greater in elevation than the office building, with a southern branch pushing past the west wall of the office building and commencing to exit from the southern domain boundary into the parking lot. The northern extent of the LFL footprint has developed just midway of the last after-reactor. Westward development of the cloud has just reached the northeast corner of the works building with the edges of both the LFL and UFL in line with the east-west axis of R6 pushing some 20 m past R6 at somewhat less than 1 m/s.

Within 16 seconds, due to the continuing momentum of the R4 jet, the UFL envelope detaches from the eastern wall of the office block to progress also in the direction of the parking lot. The LFL southern branch fills the space between the two offices and further pushes out into the parking lot at over 8 m/s; the eastern LFL development has topped the main office block and is exiting eastward at some 4 to 5 m/s. Westward development of both envelopes now has hit the NE corner of the works office and progressed westward some 8 m along its northern wall in the case of the LFL.

By 19 seconds, the LFL envelope at ground level has progressed westward some 20 m along the works office northern wall with the UFL cloud only 8 m behind. The northern development of the LFL envelope has only just reached within 22 m of the laboratory as a rather flattened pancake-shaped cloud. Both the LFL and UFL envelopes have pushed southward out into the parking lot; the UFL cloud has become completely detached from the main office block and slides along the eastern wall of the works office. The LFL envelope continues its eastern progression over the top of the main office block and around behind sections 25A and 7, exiting eastward at some 4 to 6 m/s.

In the sequence of frames following 19 seconds, pseudo-steady state has developed for the southern and easternmost exiting domain discharges; there is a strong UFL and LFL ground jet into the parking lot, along with a less strong, but volumetrically greater, one at the LFL to the east channeled by the north wall of the main office building. Aside from these two discharges to the west, both the LFL and UFL continue to enlarge with little northern development.

42.4.8 Discussion of CFD Results

Of the permanent staff of 550 employed by the company, approximately 70 of these were on-site June 1 (Westgate, 1975) . There were 28 fatalities in the explosion; of these, 18 individuals were in the control room at the time as well as 3 each in the gate house and warehouse/flaking plant (Humberside Police, 1974). In the laboratory (separated by less than 12 m from the control room, Fig. 42.2) there were eight survivors who directly witnessed the events prior to the explosion; from what they saw and heard they were able to appreciate the threat of the observed escaping cyclohexane and flee. Other witnesses, farther away, likewise directly observed the developing vapor cloud, the resultant fires, and the explosion.

In this section the eyewitness accounts of developments are briefly compared to the results of the CFD simulations of events. Additionally, site examinations of the explosion damage and fire evidence (Secretary of State for Employment, 1975; Sadee et al., 1977; Gugan, 1978; Roberts and Pritchard, 1982) and other witness statements strengthen the case for an initial single discharge from R4, followed by further follow-on occurrences that indicated that the pipe bridge failure was by a two-step process and not the single-stage event accepted by the Court.

Eyewitness Evidence. Of the eight survivors from the laboratory, seven gave evidence. Of these, five were specific in the description of a *slowly* developing vapor cloud moving to the west. This cloud was described as being about 1.5 to 2 m high and moving at 5 to 6 m/s along the ground across the clear space between the laboratory and the works office. The origin of the vapor was described as either being near the R4 reactor or its base or at least between the two (R4 and R6) reactors. *None* of the witnesses described a northward developing cloud. One described debris being thrown *up* into the air very early into the event.

Others, one about 90 m east and some 60 m north of the main office building, described a cloud of dust and smoke coming round the southern end of Section 27 (Colquhoun, 1974). Another, some 500 m to the west, observed the development of the cloud from its initiation as a ''whisper of 'steam' '' to its enlargement into a ''roaring'' jet going up river (i.e., south) and ending up ''like a fog'' across the car park (Ayre, 1974).

Various off-site witnesses, e.g., King (1974), about 500 m away, reported seeing ''dirty steam'' going up into the air, followed by ''what appeared to be an explosion that blew vapor

sideways *into* the works'' and then the major explosion; Dickinson (1974), about 200 m away, saw a flash like a large ''creamy colored torch'' coming towards him (i.e., eastward) before the explosion.

Physical Evidence. The enormity of the disaster can only be appreciated by reference to the photographs included in references (Secretary of State for Employment, 1975; Sadee et al., 1977; Gugan, 1978; Roberts and Pritchard, 1982) and others available in reports prepared in the investigation. Photographs from the press, particularly those taken by the Scunthorpe *Evening Telegraph,* reveal the extent of the destruction especially out into the car park south of the offices where most automobiles were completely crushed (Fig. 42.7).

The main and works office buildings were totally destroyed, as were the laboratory and main control room. The 0.4-m-thick concrete second floor of the southeast corner of Section 27 was displaced downwards (Roberts and Pritchard, 1982), indicating an aerial flammable cloud at this location. A tanker truck (cf. Fig. 42.7) located about 150 m east of the southern end of Section 27 was completely crushed by an overpressure estimated to be about 1 MPa (Gugan, 1976). A manhole cover located on the roadway nearly in front of the main office building and midway between the gate house and section 25A was broken by a similar overpressure (Gugan, 1976).

Physical damage to steel chemical plant components, such as reactors and strong pressure vessels located in sections 25A, 7, and 27, and closest to the main office building, exhibited crushing of their skirts or bases, which indicated overpressures on the order of 1 MPa. R5, located in the waste ground north of the works office, only exhibited a crushed skirt; the upper and weaker cylindrical section of which was uncrushed (cf. Plate 7 in Secretary of State for Employment, 1975). Similar crushing was also evident on the base of R6 but not the upstream reactors (cf. Plate 8 in Secretary of State for Employment, 1975). Process columns to the southeast in Sections 25A, 7 and 27 exhibited considerable crushing at a variety of elevations (e.g., Fig. 42.6; Plate 8 in Secretary of State for Employment, 1975, sections 25A and 27; and Fig. 2 in Roberts and Pritchard, 1982). This damage is consistent with the explosion of both ground-level (around R5 and R6) and elevated flammable clouds. Pressures sufficient to crush the bases of the reactors can only be obtained with the detonations of fuel drop-air vapor clouds (Fishburn et al., 1981; CCPS, 1994; Hoiset et al., 2000). Pressures in *closed* vessel deflagrations do not normally exceed 0.8 MPa.

That only the southern and southeast outer perimeter of plant appeared to have been subjected to such great pressures indicates that the initial extent of the fuel air cloud had not penetrated extensively into the northern sections of the plant such as would have been the result of the simultaneous dual-bellows failure scenario. Furthermore, the determined center of the explosion, just immediately north of the main office building, and stated to have been at an elevation of about 20 to 30 m (Sadee et al., 1977), coincides closely with the cloud development and its center of mass for the R4-only discharge.

Detonations of unconfined fuel-air clouds require significant ignition energy (Fishburn et al., 1981; CCPS, 1994), thus requiring, perhaps, the prior gas explosion (Harris, 1983) of the main office and/or the works office building to act as a precursor or trigger for the detonation.

Ionospheric measurements made in the close range (Jones and Spracklen, 1974) indicated that there might have been a precursor, or smaller disturbance, to the main explosion such as could have occurred with one or both of these buildings exploding. Photographs of the rubble and debris of both (Secretary of State for Employment, 1975; Sadee et al., 1977) suggest that an interior explosion occurred here first followed by the major blast. Far-range ionospheric and seismic measurements were less detailed (Grover, 1974).

The fact that all eight of the laboratory personnel saw *only* the development of a westward-moving cloud (along with the noise and other activity, some of which is noted in Table 42.1) and appreciated the threat to themselves, whereas the 18 control room staff apparently did not see anything to warn them of their great danger, indicated also that there could not

have been an extensive fuel cloud within the northern portions of sections 25A and 7 prior to the explosion.

42.4.9 Summary of the Results of the CFD Simulations

There are clear indications from the previous material that if there had been the simultaneous discharge from two reactors, as required by the Court of Inquiry, *both* the laboratory and control room staff should have appreciated the threat and been able to escape. In addition, blast damage to the northern portions of sections 25A and 7 should then have been more extreme since this northerly developing cloud should also have exploded.

This CFD analysis, coupled with the eyewitness and physical evidence, unquestionably supports the case for a two-stage failure of the pipe bridge. Such a failure only allows for an initial discharge from reactor R4 prior to the main explosion and thus a much smaller release than the 40 to 60 tons that had been previously attributed to the event (Secretary of State for Employment, 1975; Sadee et al., 1977; Gugan, 1978; Roberts and Pritchard, 1982; Bjerketvedt et al., 1997).

The facts support the case that the major explosion may have been caused by a blast in the main office building, the works office building, or both and that this may have been the trigger to the detonation of the cloud as evidenced by the physical damage and according to some observers. If true, this is one of a very few genuine UVCE detonations.

Since, as outlined earlier, flow-induced fatigue failure of the upstream bellows is here thought to be the initiating event, it is worthwhile to review the concerns of the Court on these matters. The only serious questioning was raised by Dr. Pope, Deputy Chair of the Court, in his questions of Dr. Foley (Foley, 1974d). Drs. Gill and Kitching (Gill, 1974; Kitching, 1974) as well as Dr. Ryder (Ryder, 1974) also raised concerns regarding flow-induced and other vibrations and fatigue. Dr. Foley had earlier stated that ''detecting fatigue failure in thin sheets is difficult'' (Foley, 1974e). To determine evidence for fatigue, over 26 m of failure surface would have had to have been carefully examined; by Dr. Foley's own statements this inspection was only made by ''eye and a small lens'' and thus the possibility of fatigue, especially at the interior tear in the upstream B4 bellows, cannot be ruled out. Indeed, the earlier unexplained consumption of nitrogen (Secretary of State for Employment, 1975) may have been as a result of several small existing cracks that caused the losses and then suddenly, due to fatigue damage accumulation, joined up to form the tear and thus commence the disaster.

The two CFD simulations of the possible accidental cyclohexane releases in the Flixborough disaster permit the following conclusions:

- In both cases, the R4 discharge results in ground-level vapor clouds that exit to the east, from around the southern end of sections 25A and 7, and to the south as a jet channeled between the works and main office buildings out into the parking lot.
- As well, both instances exhibit conspicuous vertical cloudlike accumulations near the southern ends of sections 25A, 7, and 27 and located on the determined focus of the blast.
- Only in the case of the single discharge from R4 is a significant westward development of the ground-level cloud displayed that corresponds to witness recollections.
- In the situation with the two simultaneous discharges, there is an extremely strong split jet (from R6) that develops into a rapidly northward moving ground-level cloud, with little westward progression. This cloud reaches the laboratory and control room areas in less than 12 seconds.
- On the basis of eyewitness reports from the laboratory technicians, who were able to escape the building before the explosion, as well as physical examinations made after the accident, it is concluded that the cause of the accidental release must have been a two-stage event,

initiated by a release from only the upstream, or R4, reactor. The initiator for this could have been a release through fatigue-generated cracks in the R4 bellows, leading to the collapse of the bridging pipe as described here.

- Further, it is possible, based upon the sizes and distributions of the vapor cloud produced, that the precursor event triggering the detonation of the cloud was a confined gas explosion that took place in either the main office or the works office or both together.

Finally, it is concluded that only about 10 to 16 tons of cyclohexane were involved in the explosion and not the 30 to 60 tons previously attributed to the event.

42.5 CONCLUSION

Finite-element and computational fluid dynamics analyses of the accident at the NYPRO Works at Flixborough have been conducted. The results suggest that the cause of the catastrophe was flow-induced fatigue of one of the bellows forming the bypass assembly that resulted in the initiation of a complex sequence of events that released only 10 to 16 tons of cyclohexane to form an unconfined vapor cloud that was detonated.

42.6 DEDICATION

It is hoped that this work may provide closure for the families of the individuals who lost their lives, and in particular remove the stigma of inappropriate action from the process control technicians killed in the event.

42.7 ACKNOWLEDGMENTS

Many individuals have contributed to the preparation of this work. Specifically, the staff at the Health and Safety Laboratory Library in Sheffield, and in particular Linda Heritage, are thanked for their help in making the Minutes of Proceedings of the Court of Inquiry and many other documents and reports dealing with the disaster available over an extended period of time; C. E. Nicholson gave permission to reference many of the SMRE and other reports available. The Scunthorpe *Evening Telegraph,* and in particular Ms. Jackie Cole, provided access to many photographs and material from their archives dealing with their staff's coverage of the accident and its aftermath. Professors T. B. Jones and Terry Robinson of the University of Leicester gave freely of their time to explain and elaborate on the ionospheric effects of the Flixborough explosion. Dr. John I. Cox provided details of his precis of the statements and reenactments of eyewitness made for the Inquiry. Ralph King and his colleague, Ronald Hirst, have provided further details regarding what influence water in the reactors may have had on the accident; the HSE are currently reporting on experiments to evaluate this. The personnel at the BBC Film Archive Unit in London assisted in the review of the background video and cine film records for the event. BBC North, and especially Christine Hamill and *Close-up North* series producer Ian Cundall made arrangements for an interview with one of the eyewitnesses, Brian Pettitt, and prepared a program historically reviewing the event and its consequences. My colleagues at the University of New Brunswick and many graduate students have all substantially contributed through discussion, critiques, and other studies. D. M. Tan conducted the ANSYS finite element (FEM) analyses and

assisted in the preparation of the Tecplot movies of the Flomerics CFD and the FEM results. Any errors and omissions are this author's alone.

42.8 REFERENCES

Ale, B. J. M., and F. Bruning. 1980a. "Unconfined Vapour Cloud Explosions," Letter, *The Chemical Engineer*, vol. 352, pp. 47–49.

Ale, B. J. M., and F. Bruning. 1980b. "Unconfined Vapour Cloud Explosions," Letter of reply, *The Chemical Engineer*, vol. 358, p. 494.

Amtec Engineering Inc. 1996. *Tecplot User's Manual*, version 7, Bellevue, WA.

ANSYS. 1994. Swanson Analysis Systems Inc., Houston, PA.

Artingstall, G. 1974. *Appraisal of the Damage in the Reactor Vessels in Section 25A,* Report No. 4, Part I, Safety in Mines Research Establishment (SMRE), September 11.

Au-Yang, M. K. 1999. "Common Mistakes and Misconceptions in Flow-Induced Vibration and Coupled Fluid-Structural Dynamics Analysis," *ASME PVPD-29*, pp. 6.1–6.17.

Ayre, E. 1974. Minutes of Proceedings at the Court of Inquiry; into the disaster which occurred at Nypro (UK) Ltd., Flixborough, Thirty-fourth Day, November 15.

Ball, J. G. 1975. "After the Flixborough Report: Do We Know the Real Truth?" *Process Engineering*, vol. 56, no. 12, pp. 39–46.

Ball, J. G. 1976. "Was This What Caused the Flixborough Explosion?" *Process Engineering*, vol. 57, no. 1, pp. 53–60.

Batstone, R. J. 1975. "Description and Results of Bellows Test Program and 20″ Dog Leg Pipe Tests," Cremer and Warner Report No. 7, January 7.

Bjerketvedt, D., J. R. Bakke, and K. van Wingerden. 1997. "Gas Explosion Handbook," *Journal of Hazardous Materials,* vol. 52, pp. 1–150.

Butler, P. 1975. "The Lessons to Be Learned from the Flixborough Enquiry," *The Engineer* (*GB*), vol. 241, no. 6247, pp. 20–24.

Carter, B. 1974. Minutes of Proceedings at the Court of Inquiry; into the disaster which occurred at Nypro (UK) Ltd., Flixborough, Fourth Day, September 12.

Center for Chemical Process Safety (CPPS). 1994. *Guidelines for Evaluating the Characteristics of Vapor-Cloud Explosions, Flash Fires, and BLEVEs,* American Institute of Chemical Engineers, New York, App. F, pp. 363–382.

Colquhoun, D. C. 1974. Minutes of Proceedings at the Court of Inquiry; into the disaster which occurred at Nypro (UK) Ltd., Flixborough, Third Day, September 11.

Cottrell, A. H., and P. R. Swan. 1974. "A Metallurgical Examination of the Eight-Inch Line," *The Chemical Engineer*, April, pp. 266–274.

Cox, J. I. 1976b. "Flixborough—Some Additional Lessons," *The Chemical Engineer*, vol. 387, pp. 353–358.

Dickinson, J. 1974. Minutes of Proceedings at the Court of Inquiry; into the disaster which occurred at Nypro (UK) Ltd., Flixborough, Second Day, September 10.

Expansion Joint Manufacturers Association (EJMC). 1993. *Standards for the Expansion Joint Manufacturers Association, Inc*., 6th ed., EJMA, Tarrytown, NY.

Fishburn, B., N. Slagg, and P. Lu. 1981. "Blast Effect from a Pancake Shaped Fuel-Drop-Air Cloud Detonation (Theory and Experiment)," *Journal of Hazardous Materials,* vol. 5, pp. 65–75.

Flomerics Ltd. 1994. *FloVent Reference Manual,* Document No. FloVent/RM/0994/1/0, Flomerics Ltd., Surrey, U.K.

Foley, J. H. 1974a. *Metallurgical Examination of the Damaged Pipes from Section 25A,* Report no. 1, Part I, Safety in Mines Research Establishment (SMRE), September 10.

Foley, J. H. 1974b. Minutes of Proceedings at the Court of Inquiry; into the disaster which occurred at Nypro (UK) Ltd., Flixborough, Thirty-third Day, November 14, pp. 34–35.

Foley, J. H. 1974c. Minutes of Proceedings at the Court of Inquiry; into the disaster which occurred at Nypro (UK) Ltd., Flixborough, Thirty-fourth Day, November 15.

Foley, J. H. 1974d. Minutes of Proceedings at the Court of Inquiry; into the disaster which occurred at Nypro (UK) Ltd., Flixborough, Thirty-seventh Day, pp. 26–27.

Foley, J. H. 1974e. Minutes of Proceedings at the Court of Inquiry; into the disaster which occurred at Nypro (UK) Ltd., Flixborough, Thirty-seventh Day, p. 21, para 5.

Foley, J. H., and C. E. Nicholson. 1974. *Metallurgical Examination of the Damaged Pipes from Section 25A,* Report no. 1, Part III, Safety in Mines Research Establishment (SMRE), November 8.

Fu, W. B., and J. A. Eyre. 1974. ''Unconfined Vapor Cloud Explosions,'' Letter, *The Chemical Engineer*, vol. 359/360, p. 368.

Games, G. A. C., and D. Waterhouse. 1974. *Construction of and Tests on a Reconstructed Bridging Pipe Assembly,* Report no. 2, Part II, Safety in Mines Research Establishment (SMRE), November 10.

Gill, S. S. 1974. Minutes of Proceedings at the Court of Inquiry; into the disaster which occurred at Nypro (UK) Ltd., Thirty-seventh Day, pp. 51–52.

Goodchild, M. B. 1975. Minutes of Proceedings at the Court of Inquiry; into the disaster which occurred at Nypro (UK) Ltd., Flixborough, Fifty-fourth Day, January 24, pp. 24–26.

Gromles, M. A. 1984. ''A Simple Approach to Transient Two-Phase Level Swell,'' in Multi-phase Flow and Heat Transfer III, Miami Beach, FL, vol. 1, pp. 527–538.

Grover, F. H. 1974. *Infrasonic and Seismic Wave Records from the Flixborough and St. Bridget Explosions,* AWRE Report 046/74.

Gugan, K. 1974. Minutes of Proceedings at the Court of Inquiry; into the disaster which occurred at Nypro (UK) Ltd., Flixborough, Thirty-ninth Day, p. 17, November 22.

Gugan, K. 1976. ''Flixborough—A Combustion Specialist's View,'' *The Chemical Engineer*, pp. 341–352.

Gugan, K. *Unconfined Vapor Cloud Explosions,* IChemE, Rugby.

Gugan, K. 1980a. ''Unconfined Vapor Cloud Explosions,'' Letter of reply, *The Chemical Engineer*, vol. 358, pp. 491–493.

Gugan, K. 1980b. ''Unconfined Vapor Cloud Explosions,'' Letter of reply, *The Chemical Engineer*, vol. 359/360, p. 567.

Gugan, K. 2000. ''Flixborough Kicking,'' Letter, *The Chemical Engineer*, May 25, p. 30.

Harris, R. J. 1983. *The Investigation and Control of Gas Explosions in Buildings and Heating Plant,* E & FN Spon, London (in association with British Gas).

Harry, L. 1974. Minutes of Proceedings at the Court of Inquiry; into the disaster which occurred at Nypro (UK) Ltd., Flixborough, Third Day, September 11.

Hoiset, S., B. H. Hjertager, T. Solberg, and K. A. Malo. 2000. ''Flixborough Revisited—An Explosion Simulation Approach,'' *Journal of Hazardous Materials*, vol. 77, nos. 1–3, pp. 1–9.

Humberside Police. 1974. Explosion, Nypro (UK) Ltd., June 1.

Jakubauskas, V. F., and D. S. Weaver. 1998a. ''Transverse Vibrations of Bellows Expansion Joints. Part I: Fluid Added Mass,'' *Journal of Fluids and Structures*, vol. 12, pp. 445–456.

Jakubauskas, V. F., and D. S. Weaver. 1998b. ''Transverse Vibrations of Bellows Expansion Joints. Part II: Beam Model Development and Experimental Verification,'' *Journal of Fluids and Structures*, vol. 12, pp. 457–473.

Jones, T. B., and C. T. Spracklen. 1974. ''Ionospheric Effects of the Flixborough Explosion,'' *Nature*, vol. 250, pp. 719–721.

King, E. 1974. Minutes of Proceedings at the Court of Inquiry; into the disaster which occurred at Nypro (UK) Ltd., Flixborough, Second Day, September 10.

King, R. 1975. ''Flixborough-Role of Water Re-examined,'' *Process Engineering*, September, pp. 69–72.

King, R. 1977. ''Latent Superheat—A Hazard of Two-Phase Liquid Systems,'' *Chemical Process Hazards,* IChemE Symposium Series no. 49, pp. 139–145.

King, R. 1999. ''Flixborough, 25 Years on,'' in *Process Engineering*, June, pp. 27–28.

King, R. 2000. ''Flixborough: Re-Open Public Inquiry,'' Letter, *The Chemical Engineer*, May 25, p. 30.

Kitching, R. 1974. Minutes of Proceedings at the Court of Inquiry; into the disaster which occurred at Nypro (UK) Ltd., Flixborough, Thirty-seventh Day, pp. 51–52.

Kletz, T. 2000. ''Flixborough, No Whitewash,'' Letter, *The Chemical Engineer*, April 20, p. 18.

Leclude, J., and J. E. S. Venart. 1996. ''Single and Two-Phase Discharge from a Pressurized Vessel,'' *Revue Generale du Thermique,* vol. 35, pp. 503–516.

Leclude, J., and J. E. S. Venart. 1997. ''Determination of the Amounts Discharged in the Flixborough Disaster,'' unpublished work, University of New Brunswick.

Marshall, H. 1974. Official Statement to Humberside Police, H Division, Scunthorpe, June 9.

Miller, K. J. 1999. Private communication, March 30.

National Institute for Standards and Technology (NIST). 1990. Standard Reference Database 4; Thermophysical Properties of Hydrocarbon Mixtures, Program Supertrapp, version 1.07, NIST, Gaithersburg, MD.

Newland, D. E. 1964. ''Buckling of Double Bellows Expansion Joints under Internal Pressure,'' *Journal of Mechanical Engineering Science,* vol. 6, pp. 270–277.

Newland, D. E. 1976. ''Buckling and Rupture of the Double Bellows Expansion Joint Assembly at Flixborough,'' *Proceedings of Royal Society of London,* series A, vol. 351, pp. 525–549.

Phillips, H. 1981. ''Unconfined Vapour Cloud Explosions: A New Look at Gugan's Book,'' *The Chemical Engineer*, vol. 369, pp. 286–287.

Rajaratnam, N., and M. R. Chamani. 1995. ''Energy Loss at Drops,'' *Journal of Hydraulic Research*, vol. 33, pp. 373–384.

Ramier, S., and J. E. S. Venart. 2000. ''Boiling Liquid Expanding Vapour Explosions: Dynamic Repressurization and Two-Phase Discharge,'' in *Hazards XV,* IChemE Symposium Series no. 147, Rugby, pp. 527–537.

Roberts, A. F., and D. K. Pritchard. 1982. ''Blast Effect from Unconfined Vapour Cloud Explosions,'' *Journal of Occupational Accidents,* vol. 3, pp. 231–247.

Ryder, D. A. 1974. Minutes of Proceedings at the Court of Inquiry; into the disaster which occurred at Nypro (UK) Ltd., Flixborough, Thirty-seventh Day, 1974, pp. 57–58.

Sadee, C., D. E. Samuels, and T. P. O'Brien. 1977. ''The Characteristics of the Explosion at the Nypro (UK) Flixborough Plant on 1 June 1974,'' *Journal of Occupational Accidents,* vol. 1, pp. 203–235.

Secretary of State for Employment. 1975. *The Flixborough Disaster*, HMSO, London.

Snedden, N. W. 1985. ''Analysis and Design Guidance for the Lateral Stiffness of Bellows Expansion Joints,'' *Thin-Walled Structures,* vol. 3, pp. 145–162.

Swan, R. 2000. ''This Is Beginning to Look Like a Cover-up,'' Editorial, *The Chemical Engineer,* April 6, p. 2.

Teng-yang, R., K. F. Sollows, and J. E. S. Venart. 2000. ''Froude Modeling of the Flixborough 'Bypass' Pipe,'' *Hazards XV,* IChemE Symposium Series no. 147, Rugby, pp. 139–154.

Venart, J. E. S. 1999. ''Flixborough: A Final Resolution?'' in INTERFLAM'99, ed. S. Grayson, vol. 1, pp. 257–272.

Venart, J. E. S., and D. M. Tan. 2000. Flixborough; Twenty-five Years after; the Final Resolution?'' in *Proceedings of ICPVT-9,* Sydney, April 9–14, vol. 2, pp. 525–539.

Warner, F. 1975. ''The Flixborough,'' *Chemical Engineering Progress*, vol. 71, no. 9, pp. 77–84.

Warner, F., and D. E. Newland. 1975. ''Flixborough Explosion—Mechanical Engineering Provides the Key,'' *Chartered Mechanical Engineer* (*GB*), June, pp. 76–81.

Weaver, D. S., and P. Ainsworth. 1989. ''Flow Induced Vibration in Bellows,'' *ASME Journal of Pressure Vessel Technology,* vol. 111, pp. 402–406.

Westgate, K. 1975. ''Flixborough—the Human Response,'' University of Bradford, Disaster Research Unit, Occasional Paper no. 7, January (reprinted September 1976).